

Uganda, Kenya, Tanzania, South Sudan, Democratic Republic of Congo, Sudan, Eritrea, Ethiopia, and Egypt. The climate of the Nile Basin is characterized by a strong latitudinal wetness gradient (Camberlin, 2009). There is a spatially contrasted distribution of mean annual rainfall over the Nile Basin. About 28 % of the basin receives less than
 5 100 mm annually. Whereas some parts experience hyper-arid conditions, substantial area exhibits sub-humid conditions. Rainfall in excess of 1000 mm is restricted mainly to the equatorial region and the Ethiopian highlands. From northern Sudan all across Egypt, rainfall is negligible (below 50 mm except along the Mediterranean coast). This general distribution reflects the latitudinal movement of the inter-tropical convergence
 10 zone (ITCZ) which never reaches Egypt and northern most Sudan, stays only briefly in central Sudan and longer further south (Camberlin, 2009).

The stationarity of our climate system for any extended period of time is highly unlikely. Whilst change in global climate is hypothetically ascribed to increase in greenhouse gas leading to observed trends in temperature and precipitation (Intergovernmental Panel on Climate Change, IPCC, 2001), annual variability may be attributed to large scale ocean–atmosphere interactions (Fowler and Archer, 2005). According to
 15 Gleick and Adams (2000), climate variability now-a-days is attracting a major concern by water resources managers and policy decision makers. For only the year 2014, a number of studies related to climate variability have been conducted examples of which include Casanueva et al. (2014), Kummu et al. (2014), Moges et al. (2014),
 20 Nachshon et al. (2014), Seiller and Ancitiln (2014), Trambauer et al. (2014), and Verdon-Kidd et al. (2014). Climate variability appears to have a very marked effect on many hydrological series (Kundzewicz and Robson, 2004). Among all the atmospheric variables, variability in rainfall is a critical factor in determining the spatiotemporal influence
 25 of the climate system on hydrology and related water management applications.

Annually, extreme rainfall and associated flooding events inflict severe damage to public life and property in many parts of the world. This is typical to various regions of the Nile Basin. Areas close to the Lake Victoria and generally low-lying parts of the Lake Victoria Basin are characterized by episodes of floods, for instance, downstream

11947

of River Nzoia and River Nyando, around Budalang'i and Kano plains (Gichere et al., 2013). Heavy rainfall events over Khartoum and Atbara led to severe flooding in Sudan during the August–September 1988 (Sutcliffe et al., 1989). According to Nawaz
 5 et al. (2010), the prolonged drought in the Greater Horn of Africa that ended in 2005 was followed by severe flooding in August 2006. In the history of flooding in the Nile Basin, Ethiopia, Tanzania, Kenya, Sudan and Uganda are the most affected countries in terms of the average number of flooding occurrences (Kibiyi et al., 2010). The flood
 10 damages in the Nile Basin are exacerbated by the already existing crisis of very frenzied poverty associated with high population growth of its inhabitants; thus, the need for sustainable planning, design and management of risk-based water resources applications. To do so, it is important to study the historical temporal variability in rainfall, and associated possible driving forces which might be from large scale ocean–atmospheric
 15 interactions and/or anthropogenic factors. Clear representation of spatial differences in the rainfall statistics across the study area would also be very supportive.

Different methods exist for computing rainfall variability; the key ones being the Empirical Orthogonal Functions (EOF) and Autocorrelation Spectral Analysis (ASA). The EOF based method applies principal component analysis to a group of rainfall time series data to extract coherent variations that are dominant. It entails computation
 20 of eigenvectors and eigenvalues of a covariance or correlation matrix obtained from a group of original rainfall time series data. Some of the studies on rainfall of the Nile Basin that used the method of EOF include Indeje et al. (2000), Ogallo (1989), and Semazzi and Indeje (1999). According to Bretherton et al. (1992), although the EOF method is satisfactory over a wide range of data structures, it is certainly not universally optimal. The ASA (Blackman and Tukey, 1959; World Meteorological Organization
 25 (WMO), 1966) utilizes the connection of autocovariance estimation and spectral analysis by the Fourier transform. In the study area this method was applied by Nicholson and Entekhabi (1986) to assess the quasi-periodic behavior of rainfall variability in Africa and its relationship to Southern Oscillation. However in this paper, Quantile Perturbation Method (QPM) is adopted as shortly described next. The QPM is quantile

11948

3.2 Test of significance

The null hypothesis (H_0) that the observed temporal variability in the rainfall dataset in question is caused by only natural variability or randomness (i.e. there is no persistence in the temporal climate variation) was considered. To verify the said hypothesis at 5 % level of significance, nonparametric bootstrapping Monte Carlo simulations were used to test the statistical significance of the temporal variation. Some of the common approaches that exist to construct confidence intervals (CIs) in statistical hypothesis testing include Monte Carlo technique, and the Jackknife method (Tukey, 1958). Examples of Monte Carlo simulations applied in statistical modelling can be found in many researches (Beersma and Buishand, 2007; Chu and Wang, 1998; Davidson and Hinkley, 1997; Onyutha and Willems, 2013). Other statistical approaches of uncertainty assessment can be found elaborated in Montanari (2011). To derive bounds of variability using 95 % CI, nonparametric bootstrapping method (Davidson and Hinkley, 1997) was employed as follows:

1. The original full time series is randomly shuffled to obtain a new temporal sequence.
2. The new series is divided to obtain subseries each of length equal to the time slice period.
3. New temporal variation of anomalies is obtained by applying QPM to the shuffled series.
4. Steps 1, 2 and 3 are repeated 1000 times to obtain 1000 anomaly factors for each subseries.
5. The anomaly values are ranked from the highest to the lowest.
6. The limits (upper, lower) of the 95 % CI for each time moment are taken as the (25th, 975th) anomaly values.

11955

Figure 2 shows an example of annual rainfall quantile anomaly series (QPM results) for station 7. The annual rainfall series is included to visualize the pattern of the quantile anomaly values in reference to the original time series. The up and down arrows indicate periods of oscillation high, OH (1940–1955) and low, OL (1956–mid 1960s) respectively. Since the upper 95 % CI limit is up crossed by the anomaly values in the OH period, it means that the OH is statistically significant in the rainfall of the selected station.

3.3 Spatial differences in rainfall statistics

Differences between rainfall intensity at the selected stations were assessed in terms of patterns of their long-term monthly mean and temporal variability. For each month in the entire series, an average of the rainfall was calculated. By repeating the procedure for all the months, indication of which months fall in the wet or dry seasons was obtained. Graphically, similarity in the obtained patterns was compared jointly for rainfall of all the stations. The temporal patterns of anomaly (QPM results) in the rainfall of the different selected stations were also compared. This was also graphically carried out by examining the similarities in the co-occurrences of the OHs and OLs. Strong spatial differences of these rainfall statistics could indicate difference in possible driving forces of temporal variability across the study area. It can also help to indicate the period during which a particular region is characterized by dry or wet spells.

3.4 Correlation between changes in rainfall and anomalies in SLP, SST and/or climate indices

Any possible linkage of rainfall variability to large scale ocean–atmosphere interactions was sought using correlation analysis (at significance level of 5 and 1 %) under the null hypothesis H_0 “there is no correlation between the rainfall QPM results and those of the SLP, SST or climate indices”. To locate the part of the world over which the driving influence for temporal variability in rainfall over the Nile Basin originates, correlation

11956

between the regional or basin-wide annual/seasonal total rainfall QPM results and corresponding SLP or SST at each grid point was calculated. Next to the correlation with the SLP, also the correlation with SLP differences, being a measure of atmospheric circulation, was tested. For that purpose, the SLP difference were considered over
 5 any two regions with significant correlations but of opposite signs and for which it is expected that the related atmospheric circulation drives the rainfall over the region under study. The oscillation pattern of the SLP difference was compared with that of the regional/basin-wide rainfall total. To further confirm the results of the comparison, correlation analyses between the QPM results of station-based annual/seasonal rain-
 10 fall and those of climate indices were carried out. Correlations between rainfall QPM results and those of the climate indices were analyzed for further investigation.

4 Results and discussions

4.1 Spatial differences in rainfall statistics

Figure 3 shows long-term mean monthly rainfall pattern for the selected stations. It is
 15 shown that the rainfall at stations in the equatorial region (group A) exhibit bimodal pattern with the main wet season in March to May (MAM) and “short rains” in October to December (OND) (Nicholson, 1996). The main wet season over Sudan and Ethiopia (group B) occurs in the months of June to September (JJAS). For stations in Egypt (group C), it is seen that the long-term mean monthly rainfall values are far lower (and
 20 of more unclear pattern) than those in groups A and B. However, it can be seen that the wet seasons cover MAM and the period of October to February (ONDJF). Because the rainfall totals for ONDJF are larger than those for MAM, it was taken as the main wet season for variability analysis. According to Camberlin (2009), large variations in long-term mean rainfall statistics across the Nile Basin is due to its great latitudinal and
 25 longitudinal extents. Based on Fig. 3, it was possible to group the selected stations into three; those in the equatorial region (group A), Sudan and Ethiopia (group B) and

11957

Egypt (group C). Validation of the grouping of the rainfall stations was in terms of the temporal variability patterns as shown next.

Figure 4 shows temporal variability of quantile anomaly (QPM results) for annual
 5 rainfall at the different stations of each group. Just like for the long-term mean monthly rainfall, it is shown that these general patterns of the temporal variability at stations of each group are similar (Fig. 4).

For group A, the OL occurred in the late 1940s to 1950s. The OL of this period was not significant at 5% level of significance in any of the selected stations. The period from 1960 to mid 1980s was characterized by its change in annual rainfall above the
 10 reference; this OH was significant at stations 2, 4 and 7. This is consistent with the findings of Kiiza et al. (2009) that for the Lake Victoria Basin, there was a significant step jump in mean of annual rainfall in the 1960s. Generally, the oscillation patterns of the annual rainfall QPM results at stations of group A are consistent with the findings of Mbungu et al. (2012) and Nyeko-Ogiramoi et al. (2013) for the Lake Victoria Basin. For
 15 group B, generally the period 1930s to 1960 was characterized by anomalies above reference. This was significant at stations 9–11, 14–15, 19–20, 24, 26, 28, 30, and 32. Another period of OH was in the early 1920s to mid 1930s. This OH was significant at stations 18, 21–23, and 27. The period from 1960s to 1980s was below reference and this OL was significant at stations 10–13, 15, 17–21, 26–27, and 31–32. In line with this
 20 OL of the period 1960s to 1980s, Hulme (1992) found that the mean annual rainfall in the Sahel region for the decades 1970s and 1980s declined by 30%. For group C, the period of OL occurred in the late 1920s to 1930s. This was, however, based on only station 36 whose record starts in 1904. The OH occurred in the period from about 1940 to early 1950s. This was significant at stations 34–35 and 37. Though not significant at
 25 any station, OL occurred over the period of mid 1950s to 1970s. For the QPM results of rainfall in the main wet season (not shown) of each group, the stations at which there were significant OHs like for the annual rainfall (over the same period) were 2, 4 and 7 (MAM); 22–23, 26–27, and 32 (JJAS); 35–37 (ONDJF). However, there were some stations that exhibited significant OHs in the main wet season but not for the annual

11958

Acknowledgements. The research was financially supported by an IRO Ph.D. scholarship of KU Leuven.

References

- Abteu, W., Melesse, A. M., and Dessalegne, T.: El Niño Southern Oscillation link to the Blue Nile River Basin hydrology, *Hydrol. Process.*, 23, 3653–3660, 2009.
- Ahrens, B.: Distance in spatial interpolation of daily rain gauge data, *Hydrol. Earth Syst. Sci.*, 10, 197–208, doi:10.5194/hess-10-197-2006, 2006.
- Allan, R. and Ansell, T.: A new globally complete monthly Historical Gridded Mean Sea Level Pressure Dataset (HadSLP2): 1850–2004, *J. Climate*, 19, 5816–5842, 2006.
- Beersma, J. J. and Buishand, T. A.: Drought in the Netherlands – regional frequency analysis vs. time series simulation, *J. Hydrol.*, 347, 332–346, 2007.
- Beltrando, G. and Camberlin, P.: Interannual variability of rainfall in the Eastern Horn of Africa and indicators of atmospheric circulation, *Int. J. Climatol.*, 13, 533–546, 1993.
- Blackman, R. B. and Tukey, J. W.: *The Measurement of Power Spectra*, Dover Publications, New York, 190 pp., 1959.
- Bretherton, C. S., Smith, C., and Wallace, J. M.: An intercomparison of methods for finding coupled patterns in climate data, *J. Climate*, 5, 541–560, 1992.
- Camberlin, P.: Rainfall anomalies in the source region of the Nile and their connection with the Indian summer monsoon, *J. Climate*, 10, 1380–1392, 1997.
- Camberlin, P.: Nile Basin Climates, in: *The Nile: Origin, Environments, Limnology and Human Use*, *Monographiae Biologicae*, vol. 89, edited by: Dumont, H. J., Springer, Dordrecht, 307–333, 2009.
- Casanueva, A., Rodríguez-Puebla, C., Frías, M. D., and González-Reviriego, N.: Variability of extreme precipitation over Europe and its relationships with teleconnection patterns, *Hydrol. Earth Syst. Sci.*, 18, 709–725, doi:10.5194/hess-18-709-2014, 2014.
- Chiew, F. H. S.: An overview of methods for estimating climate change impact on runoff, paper presented at the 30th Hydrol. and Water Resourc. Symp., Launceston, Australia, 4–7 December, CDROM, Eng. Aust., Barton, Australian Capital Territory, 2006.
- Chu, P. and Wang, J.: Modeling return periods of tropical cyclone intensities in the vicinity of Hawaii, *J. Appl. Meteorol.*, 37, 951–960, 1998.

11965

- Davidson, A. C. and Hinkley, D. V.: *Bootstrap Methods and their Application*, Cambridge University Press, Cambridge, UK, 582 pp., 1997.
- Dirks, K. N., Hay, J. E., Stow, C. D., and Harris, D.: High-resolution of rainfall on Norfolk Island, Part II: Interpolation of rainfall data, *J. Hydrol.*, 208, 187–193, 1998.
- Diro, G., Grimes, D. I. F., and Black, E.: Teleconnections between Ethiopian summer rainfall and sea surface temperature: Part I – observation and modelling, *Clim. Dynam.*, 37, 121–131, 2010.
- FAO: FAOCLIM 2: world-wide agroclimatic data, Environment and Natural Resources, No. 5 (CD-ROM) of working papers series of FAO, Rome, Italy, 2001.
- Fontaine, B. and Janicot, S.: Wind-field coherence and its variations over West Africa, *J. Climate*, 5, 512–524, 1992.
- Fowler, H. J. and Archer, D. R.: Hydro-climatological variability in the Upper Indus Basin and implications for water resources, paper presented at S6 symposium on Regional Hydrological Impacts of Climatic Change-Impact Assessment and Decision Making (the Seventh IAHS Scientific Assembly at Foz do Iguaçu, Brazil, April 2005), IAHS Publ. 295, 2005.
- Gichere, S. K., Olado, G., Anyona, D. N., Matano, A. S., Dida, G. O., Abuom, P. O., Amayi, A. J., and Ofulla, A. V. O.: Effects of drought and floods on crop and animal losses and socio-economic status of households in the Lake Victoria Basin of Kenya, *J. Emerg. Trends in Econ. Manage. Sci.*, 4, 31–41, 2013.
- Grist, J. P. and Nicholson, S. E.: A study of the dynamic forces influencing rainfall variability in the West Africa Sahel, *J. Climate*, 14, 1337–1359, 2001.
- Goovaerts, P.: Geostatistical approaches for incorporating elevation into the spatial interpolation of rainfall, *J. Hydrol.*, 228, 113–129, 2000.
- Gleick, P. H. and Adams, D. B.: *Water: the Potential Consequences of Climate Variability and Change for the Water Resources of the United States*, Pacific Institute for Studies in Development, Environment, and Security 654 13th Street Preservation Park Oakland, 162 pp., 2000.
- Harrold, T. I. and Jones, R. N.: Downscaling GCM rainfall: a refinement of the perturbation method, paper presented at MODSIM 2003, Int. Congr. on Modell., and Simul., Townsville, 14–17 July, Modelling and Simulation Soc. of Aust. and N.Z., Canberra, Australia, 2003.

11966

Table 2. Overview of SLP, SST and related time series.

Data	Downloaded from:	Accessed on:	Resolution/period
SLP related series			
HadSLP2	http://www.esrl.noaa.gov/psd/	12 May 2014	5° × 5°, daily (1850–2013)
NAO	http://www.cru.uea.ac.uk/cru/data/nao/	29 Jan 2013	Monthly (1900–2000)
NPI	http://www.cgd.ucar.edu/cas/jhurrell/indices.data.html	29 Jan 2013	Monthly (1900–2011)
TPI	http://www.cru.uea.ac.uk/cru/data/tpi/	29 Jan 2013	Monthly (1900–2003)
SOI	http://www.cru.uea.ac.uk/cru/data/soi/	29 Jan 2013	Monthly (1900–2004)
SST related series			
HadSST2	http://badc.nerc.ac.uk/	30 May 2014	5° × 5°, daily (1850–2013)
AMO	http://climexp.knmi.nl/data/iamo_hadsst2.dat	29 Jan 2013	Monthly (1900–2012)
PDO	http://jisao.washington.edu/pdo/PDO.latest	30 Jan 2013	Monthly (1900–2011)
IOD	http://www.jamstec.go.jp/frcgc/research/d1/iod	20 Jan 2014	Monthly (1900–2003)
Niño 3	http://www.esrl.noaa.gov/psd/gcos_wgsp/Timeseries/Nino3/	29 Jan 2013	Monthly (1900–2011)
Niño 3.4	http://www.esrl.noaa.gov/psd/gcos_wgsp/Timeseries/Nino34/	29 Jan 2013	Monthly (1900–2011)
Niño 4	http://www.esrl.noaa.gov/psd/gcos_wgsp/Timeseries/Nino4/	29 Jan 2013	Monthly (1900–2012)

11973

Table 3. Correlation between rainfall and SLP differences taken at locations shown in Fig. 7.

Group-A	Annual	MAM	Group-B (continued)	Annual	JJAS
Kabale	-0.62	0.05	Nyala	-0.69	-0.71
Namasagali	-0.4	-0.6	Renk	-0.63	-0.42
Igabiro	-0.65	-0.57	Shambat-Obs.	-0.56	-0.5
Kibondo	-0.71	-0.63	Shendi	-0.88	-0.75
Ngudu	-0.53	-0.5	Talodi	-0.58	-0.63
Shanwa	-0.63	-0.55	Talodi-Min.Agric.	-0.82	-0.81
Tarime	-0.5	-0.81	Umm-Ruwaba	-0.82	-0.82
Bujumbura	-0.68	-0.61	Wau	-0.76	-0.83
Region-wide rainfall	-0.75	-0.85	Combolcha	-0.71	-0.64
Group-B	Annual	JJAS	Debremarcos	-0.79	-0.66
El-Da-Ein	-0.86	-0.78	Gambela	-0.72	-0.65
El-Fasher	-0.87	-0.63	Gore	-0.5	-0.32
El-Obeid	-0.8	-0.84	Wenji	-0.14	-0.13
En-Nahud	-0.7	-0.65	Region-wide rainfall	-0.88	-0.82
Er-Rahad	-0.56	-0.62	Group-C	Annual	ONDJF
Fashashoya	-0.4	-0.25	Asswan	-0.53	-0.2
Garcila	-0.69	-0.72	Asyut	-0.66	-0.2
Hawata	-0.55	-0.66	Helwan	-0.72	-0.59
Jebelein	-0.64	-0.55	Qena	-0.59	-0.28
Kassala	-0.84	-0.63	Region-wide rainfall	-0.72	-0.59
Kubbum	-0.79	-0.69			
Kutum	-0.85	-0.71			

11974

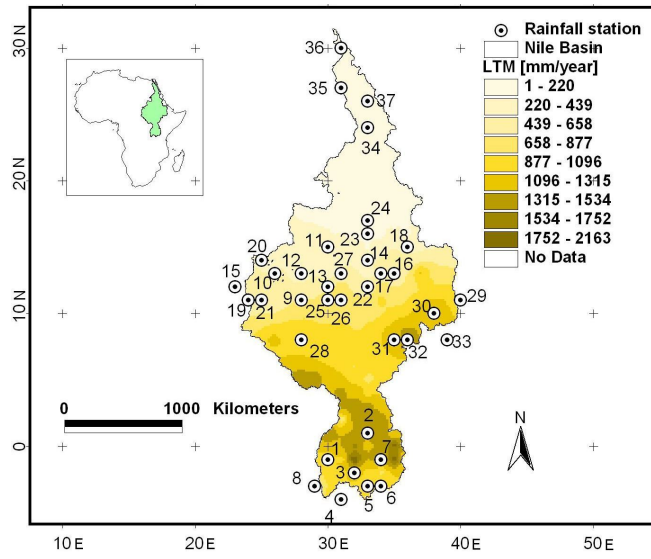


Figure 1. Locations of the selected meteorological stations (see Table 1 for details) in the Nile Basin; the background is based on the LTM.

11977

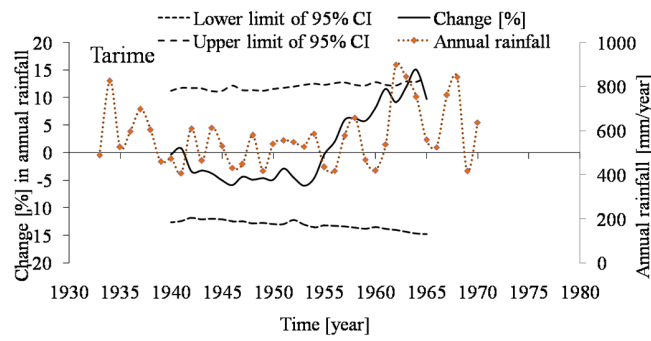


Figure 2. Annual rainfall and QPM results for a time slice of 15 years and period 1935–1970.

11978

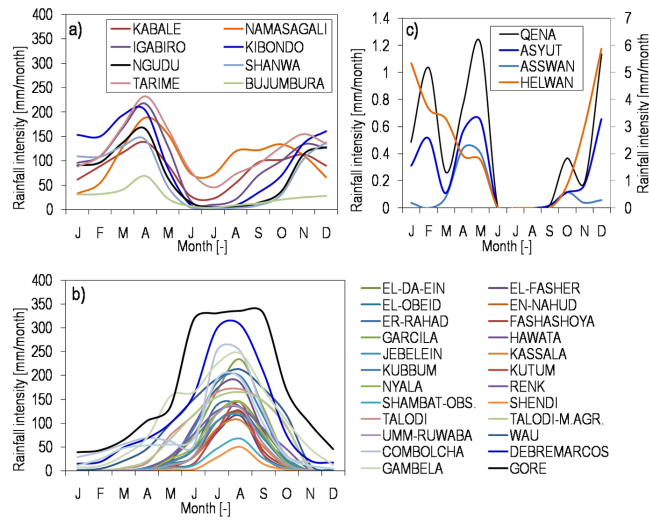


Figure 3. Long-term mean monthly rainfall pattern for group (a) A, (b) B, and (c) C.

11979

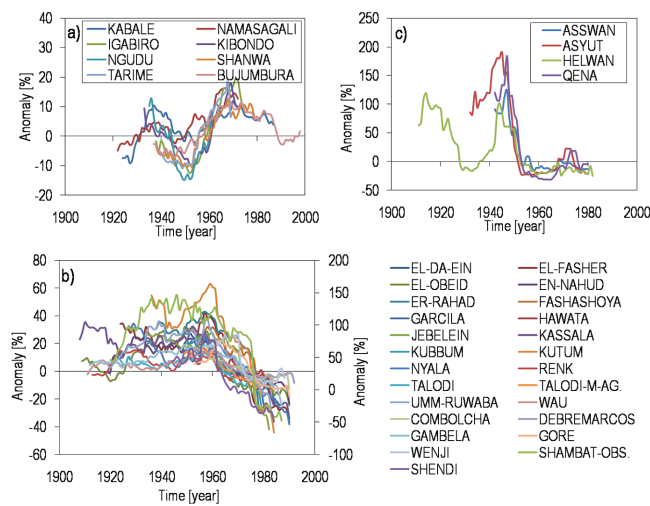


Figure 4. QPM results for annual rainfall using a time slice of 15 years and rainfall stations for group (a) A, (b) B, (c) C.

11980

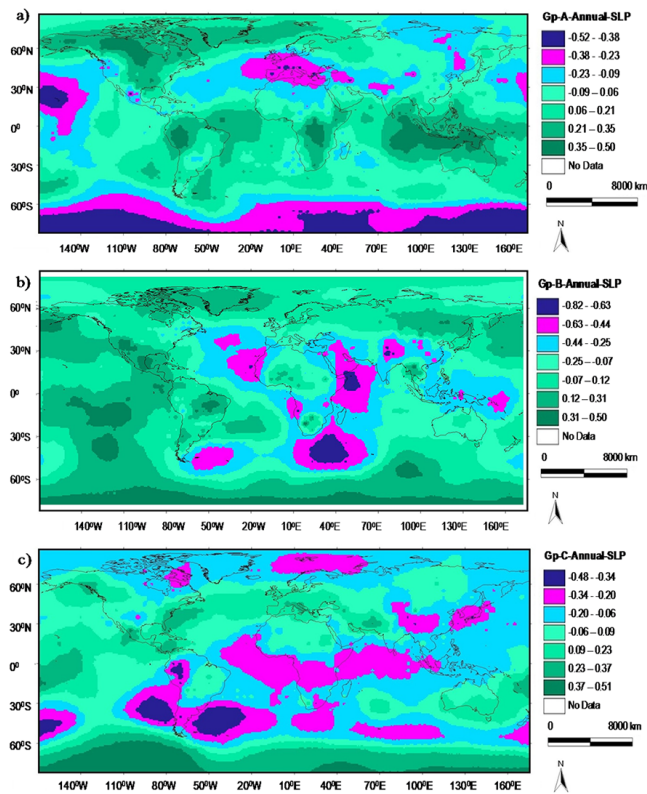


Figure 5. Correlation between anomaly in annual SLP and that in region-wide annual rainfall for group (a) A, (b) B, (c) C.

11981

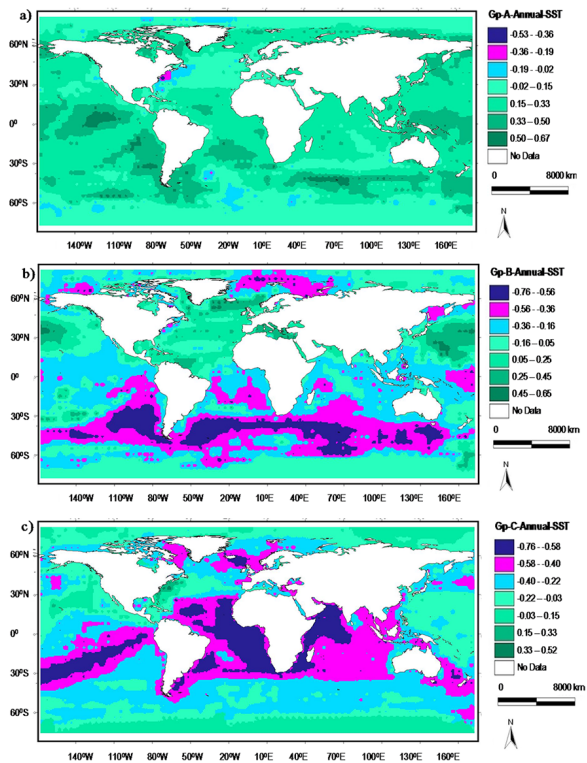


Figure 6. Correlation between annual SST and region-wide annual rainfall for group (a) A, (b) B, (c) C.

11982

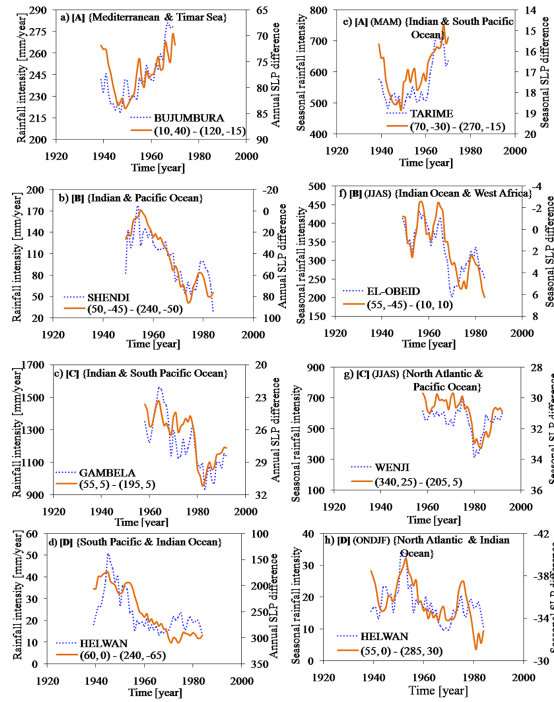


Figure 7. Annual SLP differences and rainfall at selected stations of the different groups A–C for a time slice of 5 years; the group labels are in (). The label of a legend indicates the coordinates (degree longitude and latitude) from where the SLP differences were taken. The label in { } show the locations where the coordinates are found. Annual and seasonal time scales are shown in charts (a)–(c) and (d)–(f) respectively.

11983

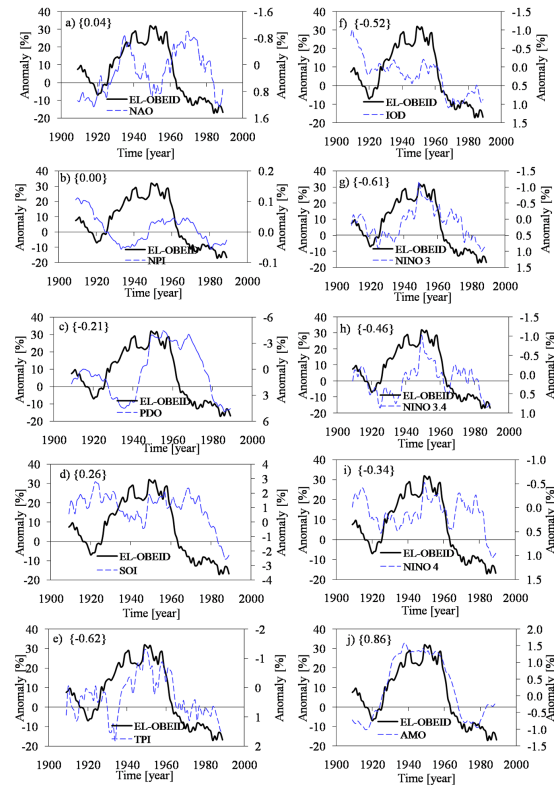


Figure 8. QPM results for annual rainfall and climate indices; the correlation coefficient between the two curves of each chart is put as label in { }.

11984

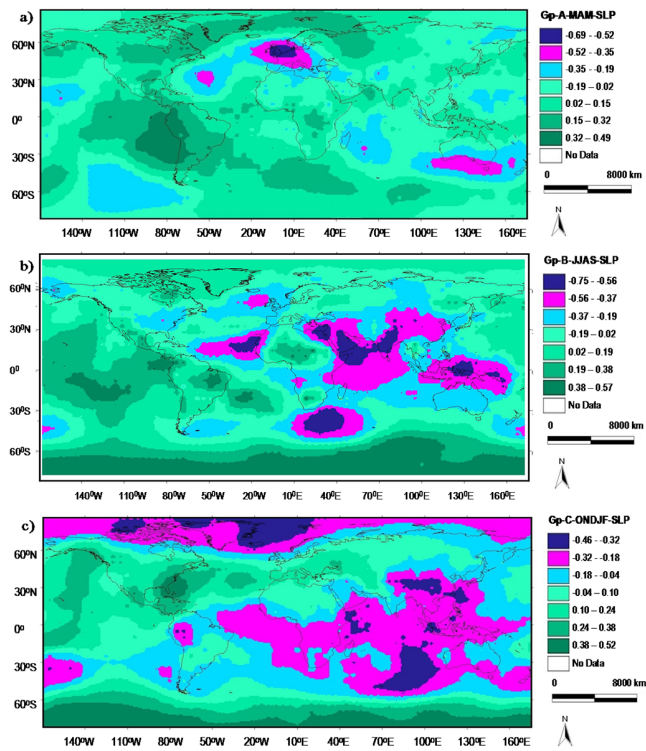


Figure A1. Correlation between season-based SLP and region-wide rainfall for group (a) A, (b) B, (c) C.

11985

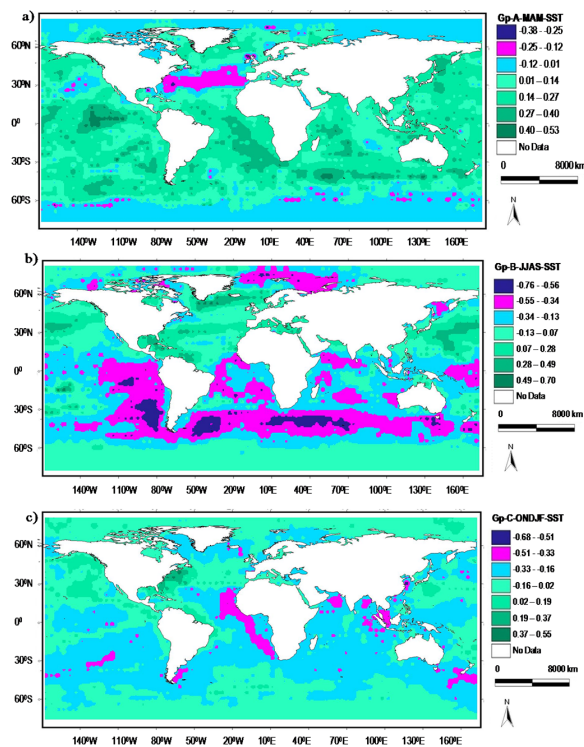


Figure B1. Correlation between season-based SLP and region-wide rainfall for group (a) A, (b) B, (c) C.

11986